Efficient Synthesis of Unimolecular Polymeric Janus Nanoparticles and Their Unique Self-Assembly Behavior in a Common Solvent

Lin Cheng,[†] Guolin Hou,[†] Jianjun Miao,[‡] Daoyong Chen,*[,†] Ming Jiang,[†] and Lei Zhu*[,‡]

Department of Macromolecular Science and The Key Laboratory of Molecular Engineering of Polymers, Fudan University, 220 Handan Rd., Shanghai 200433, China, and Polymer Program, Institute of Materials Science and Department of Chemical, Materials and Biomolecular Engineering, University of Connecticut, Storrs, Connecticut 06269-3136

Received March 3, 2008; Revised Manuscript Received August 4, 2008

ABSTRACT: In this paper, we report a facile large-scale synthesis of the "smallest" (i.e., unimolecular) polymeric Janus nanoparticles from a polystyrene-*b*-poly(2-vinylpyridine)-*b*-poly(ethylene oxide) (PS-*b*-P2VP-*b*-PEO or SVEO) triblock copolymer by efficient intramolecular cross-linking of the middle P2VP block using 1,4-dibromobutane (DBB) in a common solvent, *N*,*N*-dimethylformamide (DMF), due to effective steric shielding of PS and PEO end blocks. Size-exclusion chromatography results indicated that intramolecular cross-linking of the middle P2VP block could take place when the polymer concentration was relatively high (20 mg/mL) and/or the DBB-to-2VP molar ratio was high. Dynamic and static light scattering experiments confirmed the unimolecular form for these polymeric Janus nanoparticles. After intramolecular cross-linking, DMF changed from a good to a slightly poor solvent, as evidenced by the negative apparent second Virial coefficient for the unimolecular Janus nanoparticles determined by SLS. As a result, concentration-dependent self-assembly in DMF was observed. At low concentrations (<2.0 mg/mL), the majority of the unimolecular polymeric Janus nanoparticles existed in the unimolecular form. When the concentration gradually increased, the unimolecular polymeric Janus nanoparticles started to aggregate into supermicelles ($R_h = 50-100$ nm), where PS formed the supercore and PEO formed the corona with cross-linked P2VP nanoparticles in between. The amphiphilic nature of these unimolecular Janus nanoparticles will enable us to study programmable and hierarchical self-assembly of asymmetrically modified polymeric nanoparticles in various solvents.

Introduction

Intramolecularly collapsed single chain particles can be considered as the "smallest" polymeric nanoparticles, and they have unusual macroscopic physical properties due to their small size and polymeric nature.[1−5] For example, when blended into polymers having the same chemistry, they induced a decrease in the bulk viscosity, contrary to common solid particle filled polymeric systems as predicted by Einstein.[6] Recently, self-assembly of inorganic nanoparticles into superparticles or clusters has attracted much attention, because they have demonstrated different properties from molecularly self-assembled systems and have potential for applications including catalysis, electronic/optical materials, and drug delivery.[7] However, self-assembly of these smallest polymeric nanobuilding blocks into ordered superstructures still remain challenging because of isotropic interactions at particle surfaces. It is reported that introduction of sticky patches onto nanoparticle surfaces is an effective approach for particle self-assembly.[8,9] In particular, asymmetric decoration of nanoparticles with a hydrophilic chain at one end and a hydrophobic chain at the other end (or the smallest Janus nanoparticles) will enable programmable self-assembly into hierarchical superstructures.[10]

Since de Gennes first coined the term "Janus" for particles with distinct hemispheres of different chemical natures and predicted their unique self-assembly at oil−water interfaces in 1991,[11] Janus particles have received much attention in the past 17 years.[12] Their applications range from novel Pickering[13] emulsions for paints and coatings[14] to giant dipolar particles for electronic displays[15−17] to difunctional carriers for catalysis, sensing, and drug delivery. On the basis of particle sizes, Janus particles can be divided into micro- and nanoparticles. Recently, there have been tremendous efforts to synthesize micron-sized Janus particles with mostly spherical and other shapes using the dual-supplied spinning disk technique,[15,16] toposelective surface modification,[17−28] continuous-flow lithography,[29] microfluidic assembly,[30,31] dual-jet electrospinning,[32] and layer-by-layer self-assembly.[33]

Most research on Janus nanoparticle so far has been focused on inorganic nanoparticles. These nanoparticles can be synthesized by controlled phase separation in core−shell nanoparticles,[34,35] controlled surface nucleation from nanoparticles,[36−38] and monofunctionalization of nanoparticles via solid-state synthesis[39−46] or single DNA chain attachment.[47,48] For controlled phase separation and surface nucleation from nanoparticles, dumbbell- or snowman-shaped nanoparticles were commonly obtained.[36−38]

Instead, polymeric Janus nanoparticles have attractive advantages,[49] because they are more versatile to modification with a broad range of functional groups at the surface, and their solution behavior is much easier to tailor than that of inorganic nanoparticles. Therefore, polymeric Janus nanoparticles can be more advantageous for microemulsion stabilization, heterogeneous phase catalysis, and targeted drug delivery. One elegant method to synthesize polymeric Janus nanoparticles is to chemically cross-link spherical microdomains in the "*sphere-on-the-lamellar*" morphology of self-assembled ABC triblock copolymers. Examples are polystyrene-*b*-poly(2-vinyl pyridine)-*b*-poly(*tert*-butyl methacrylate) (PS-*b*-P2VP-*b*-P*t*BMA)[50] and PS-*b*-polybutadiene-*b*-poly(methyl methacrylate) (PS-*b*-PB-*b*-PMMA).[51−55] After deprotecting the methyl ester groups in the PMMA block to form poly(acrylic acid) (PAA), amphiphilic Janus nanoparticles were prepared and exhibited intriguing self-assembly behavior in aqueous solutions.[51,56−58] This method

* Corresponding authors. E-mail: chendy@fudan.edu.cn (D.C.) and lei.zhu@uconn.edu (L.Z.).
[†] Fudan University.
[‡] University of Connecticut.

10.1021/ma800461z CCC: $40.75
Published on Web 10/08/2008

Scheme 1. Synthesis of Unimolecular Polymeric Janus Nanoparticles and Their Self-Assembly in a Common Solvent, DMF

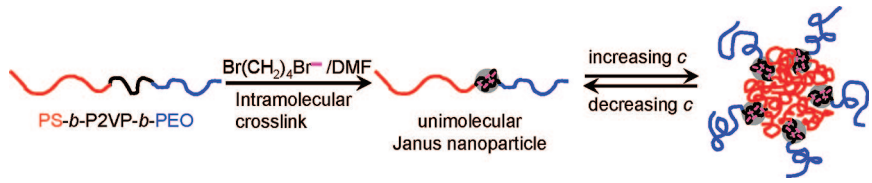

requires specific triblock copolymer compositions (short B block and relatively long A and C blocks with A ≈ C) to ensure the sphere-on-the-lamella and "*cylinder-on-the-lamella*" morphology in the bulk samples. Besides the above method, polymeric micelles with mixed corona chains, which eventually phase separated into a dipolar structure, may also be called Janus nanoparticles.[59−61] However, these polymeric Janus particles are composed of an ensemble of molecules, and the "smallest" (or unimolecular) polymeric Janus nanoparticles have not been achieved. Therefore, it is still challenging to invent a versatile way to synthesize the smallest polymeric Janus nanoparticles from ABC triblock copolymers.

In this work, a facile method utilizing chemical cross-linking-induced micellization[62] of an amphiphilic ABC triblock copolymer, namely, polystyrene-*b*-poly(2-vinyl pyridine)-*b*-poly(ethylene oxide) (PS-*b*-P2VP-*b*-PEO or SVEO), was employed to prepare, in a large scale, novel unimolecular polymeric Janus nanoparticles in a common solvent, *N*,*N*-dimethylformamide, DMF (see Scheme 1). Note that here we use the words "common solvent", because conventionally DMF is a good solvent for PS, PEO, P2VP, and quarternized P2VP (PQ2VP) homopolymers. Contrary to the traditional dilute solution approach, efficient intramolecular, instead of intermolecular, cross-linking of the middle P2VP blocks due to the steric shielding from two long end blocks enabled large-scale synthesis at a relatively high concentration (i.e., 20 mg/mL). Intriguingly, these amphiphilic unimolecular polymeric Janus nanoparticles exhibited concentration dependent self-assembly in DMF.

Experimental Section

Materials. The SVEO triblock copolymer was purchased from Polymer Source, Inc. Its absolute weight-average molecular weight (M_w) and polydispersity index (PDI) were 304 000 g/mol and 1.15, respectively, as determined by both static light scattering and multiple-detector size-exclusion chromatography (SEC) (see Figure 1 below). The number-average molecular weights (M_ns) of the PS, P2VP, and PEO blocks were determined by proton nuclear magnetic resonance (^{1}H NMR) to be 136 000, 47 500, and 80 500 g/mol, respectively, using the M_w and PDI values. 1,4-Dibromobutane (DBB) was purchased from Aldrich and used directly. DMF (Acros) was purified by reduced pressure distillation over CaH_2.

Cross-Linking of SVEO Triblock Copolymers in DMF. A predetermined amount of DBB was added using a microsyringe to 10.0 or 2.0 mL of the SVEO in purified anhydrous DMF solution with a concentration of 2.0 or 20 mg/mL, respectively. Three molar ratios of DBB-to-2VP were used, 8:1, 2:1, and 1:2. The mixture solution was degassed three times using the freeze−pump−thaw method and then vacuum sealed in an ampule. The solution was heated to either 30 or 100 °C for 2 weeks or 24 h, respectively.

Characterization Methods. Both dynamic and static light scattering (DLS and LLS) were carried out using an ALV-5000 laser light scattering spectrometer. All the solutions were filtered through 0.45 μm Millipore filters (hydrophilic Millex-LCR, PTFE) to remove dust and then kept at 25 ± 0.1 °C for at least 2 h before light scattering measurements. DLS measurements were performed at a fixed scattering angle of 90° and 15°, respectively. The $\langle R_h \rangle$ and PDI were obtained by the CONTIN program. SLS studies were conducted at a scattering-angle (θ) ranging from 15° to 150° with an angular step of 5°. The Zimm model was used for the SLS. The specific refractive index increment (dn/dc) was determined by a Jianke differential refractometer (Jianke Instrument, Ltd.) using four different concentration solutions (1.0, 2.5, 5.0, 10.0 mg/mL) of the pure SVEO and DBB-cross-linked SVEO in DMF, whose dn/dc values were determined as 0.1365 and 0.1360 mL/g, respectively.

Transmission electron microscopy (TEM) experiments were carried out on a Philips CM120 microscope operated at an accelerating voltage of 80 kV. Approximately, 5 μL of the sample solution was deposited onto a carbon-coated copper TEM grid. After the DMF was completely evaporated at room temperature, the TEM grids with samples were further dried in a vacuum desiccator for 36 h before TEM observations. The unimolecular polymeric Janus nanoparticles were stained by RuO_4 for 15 min.

Quadruple-detector [differential refractive index (RI), UV−vis, differential viscometer (intrinsic viscosity, IV), and right-angle light scattering (RALS)] SEC experiments were carried out on a Viscotek

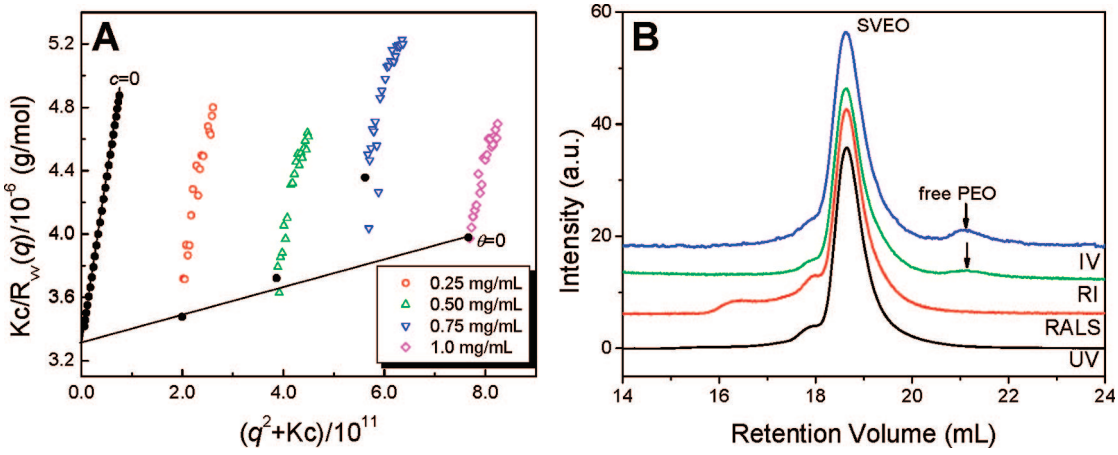

Figure 1. (A) Zimm plot for the pure SVEO in DMF. The second Virial coefficient A_2 is determined from the slope of the solid line at $\theta = 0$ to be 3.41×10^{-4} mol·cm^3/g^2. (B) Multidetector SEC curves for the pure SVEO using DMF as solvent. IV represents the intrinsic viscosity response, RI is the differential refractive index response, and RALS is the right-angle light-scattering response. The peak retention volumes for IV, RALS, and UV signals were corrected to be the same as the RI peak retention volume at 18.6 mL. Curves are overlaid for clarity.

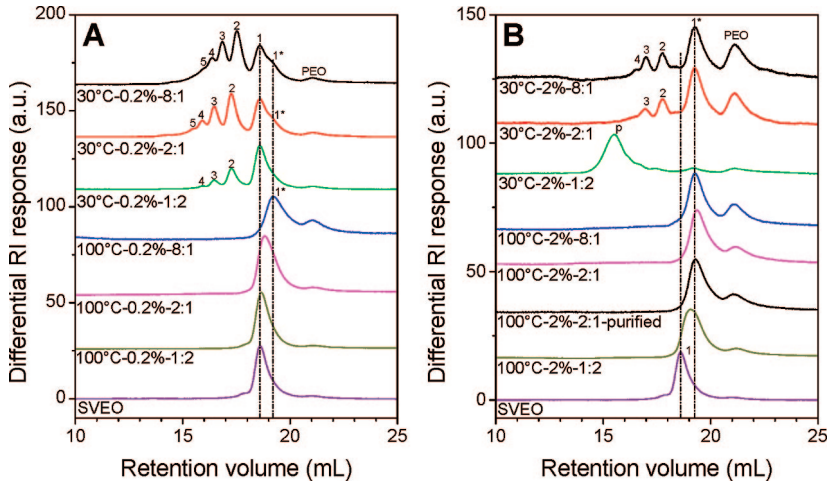

Figure 2. Differential refractive index SEC curves for the pure SVEO and DBB-cross-linked SVEO products under different reaction conditions. The concentrations of the SVEO are (A) 2.0 mg/mL and (B) 20 mg/mL, respectively.

GPCMax VE2001 instrument equipped with three Jordi polydivinylbenzene columns (Jordi FLP, Burlingham, MA) having pore sizes of 100 000, 10 000, and 1000 Å, respectively. The columns were kept at a constant temperature of 40 °C. HPLC-grade DMF (n = 1.430) was used as the mobile phase at a flow rate of 1.0 mL/min. In some experiments, the mobile phase was added with LiBr at a concentration of 0.05 M to avoid adsorption of quarternized polymers onto SEC columns. A poly(methyl methacrylate) (PMMA) standard (M_n = 750 000 g/mol and PDI = 1.12) was used to calibrate the optical constant for the multidetector calibration. The molecular weights and PDI were calculated using the OmniSEC 3.1 software.

^{1}H NMR experiments were carried out using a Bruker DMX500 spectrometer. After preparation of unimolecular Janus particles in protonated DMF, the solvent was completely evaporated in a vacuum oven. The dried sample was redissolved in DMF-d_7 for subsequent ^{1}H NMR measurements.

Results and Discussion

Molecular Characterization of the SVEO Triblock Copolymer. The absolute M_w of the starting SVEO triblock copolymer was first determined by the Zimm plot analysis using SLS (Figure 1A). Four concentrations were used, 0.25, 0.50, 0.75, and 1.0 mg/mL. After extrapolation to both $c = 0$ and $\theta = 0$, the absolute M_w was thus determined as the reciprocal intercept, i.e., 302 600 g/mol. From the slope of the fitted line at $\theta = 0$, the apparent second Virial coefficient (A_2) was determined as $A_2 = 3.41 \times 10^{-4}$ mol·cm^3/g^2. Note that the positive A_2 indicates that DMF is a good solvent for the SVEO triblock copolymer. This M_w was further confirmed by SEC results using multidetector calibration, as shown in Figure 1B. RI and IV curves showed a slight shoulder at a smaller retention volume of 17.9 mL and a weak peak at a higher retention volume of 21.1 mL. The weak peak at 21.1 mL is not detectable in the UV curve, implying that it should be a free PEO contaminant formed during the last step of anionic polymerization of ethylene oxide.[63] The content of free PEO was estimated to be 4 wt %, as calculated from the RI curve. The slight shoulder at 17.9 mL could be attributed to a higher molecular weight contaminant, and the reason for its formation is unclear. In addition, the RALS curve as well as the low-angle light scattering (LALS) curve (data not shown) showed a broad peak around 16.5 mL. This broad peak could be attributed to aggregates of the SVEO triblock copolymer in DMF. Judging from the fact that neither RI nor UV curves showed this broad peak, the concentration of these aggregates in DMF must be very low. Because light scattering is much more sensitive to larger particles, these low-concentration aggregates can be detectable by light scattering detectors. With the OmniSEC 3.1 software, the absolute M_w and PDI were calculated to be 304 000 g/mol and 1.15, respectively, using the multidetector calibration. The M_n of the SVEO was thus 264 00 g/mol. Because of its narrow molecular weight distribution, the M_ns of the PS, P2VP, and PEO blocks could be determined by ^{1}H NMR to be 136 000, 47 500, and 80 500 g/mol, respectively.

Inter- and Intramolecular Cross-Linking of SEVO by DBB in DMF. When DBB reacts with the SVEO triblock copolymer, three types of reactions are possible, namely, grafting of DBB molecules to the P2VP block and intra- and intermolecular cross-linking of the middle P2VP blocks. Depending on the concentration of the SVEO, the molar ratio of DBB-to-2VP, and the reaction temperature, these three reactions compete with each other, forming different final products. Figure 2A shows DBB-cross-linked SVEO under different reaction conditions when the polymer concentration was relatively low, e.g., 2 mg/mL or 0.2%. First, when the reaction was carried out at 30 °C, no obvious peaks (except slight shoulders) could be found at a higher retention volume than that of the pure SVEO at 18.6 mL, no matter what molar ratio of DBB-to-2VP was used. In addition to the peak at 18.6 mL (either the pure SVEO or partly DBB-grafted SVEO), multiple sharp peaks were observed at smaller retention volumes for the DBB-treated samples, indicative of intermolecular cross-linking between the SVEO chains. Presumably, they could be assigned as two-, three-, four-, and even five-chain cross-linked species. Upon increasing the molar ratio of DBB-to-2VP from 1:2 to 2:1 and 8:1, the intermolecular cross-linking became more pronounced, since the peak intensity at 18.6 mL gradually decreased. Comparing the retention volumes of the corresponding intermolecularly cross-linked species having the same number of chains, the quarternized P2VP cores for the DBB-to-2VP molar ratio of 8:1 showed a higher cross-linking density than those of 2:1, because the sample had a higher retention volume and thus a smaller hydrodynamic volume.

Second, when the reaction temperature increased to 100 °C, a sharp peak with a higher retention volume (smaller hydrodynamic volume) at 19.2 mL was observed for the DBB-treated samples when the DBB-to-2VP molar ratios were 8:1, implying that intramolecular cross-linking probably took place in a SVEO chain. When the DBB-to-2VP molar ratio was 1:2 at 100 °C, the SEC curve was almost unchanged from that for pure SVEO, indicating that the 24-h reaction time was not long enough for cross-linking to occur. When the DBB-to-2VP molar ratio was

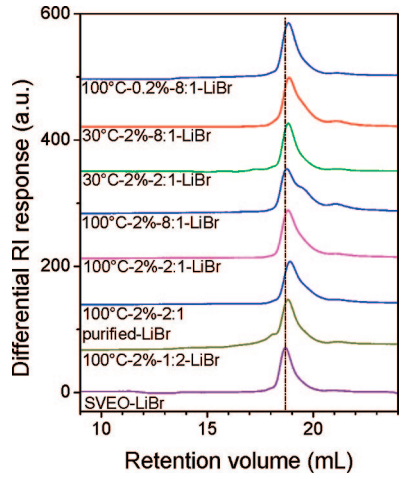

Figure 3. Differential refractive index SEC curves for the pure SVEO and DBB-cross-linked SVEO products under different reaction conditions, using 0.05 LiBr/DMF as the mobile phase.

2:1, a unimodel but slightly broadened peak was observed with a retention volume between 18.6 and 19.2 mL. This suggested that intramolecular cross-linking took place only partially among all SVEO triblock molecules. We also notice that the free PEO peak appeared to be 5 times stronger for the sample with the DBB-to-2VP molar ratio of 8:1 than for pure SVEO. This suggested that part of the intramolecularly cross-linked species (at 19.2 mL) must have been adsorbed onto the SEC columns because of its less protected structure by only one PS and one PEO block than the intermolecularly cross-linked species. To avoid preferred adsorption of intramolecularly cross-linked species onto SEC columns, LiBr was added to the DMF mobile phase at a concentration of 0.05 M, and the corresponding SEC curve is shown at the top of Figure 3. A single sharp peak with a retention volume (18.8 mL) slightly higher than that (18.7 mL) of pure SVEO was observed, demonstrating that intramolecularly cross-linked SVEO was successfully achieved.

Figure 2B shows DBB-cross-linked SVEO under different reaction conditions when the polymer concentration was relatively high, e.g., 20 mg/mL or 2%. First, when the reaction was carried out at 30 °C, peaks at a retention volume of 18.6 mL (either the pure SVEO or the DBB-grafted SVEO) completely disappeared. When the DBB-to-2VP molar ratio was 8:1 and 2:1, respectively, peaks at retention volume of 19.2 mL were observed, representing intramolecularly cross-linked SVEO. Meanwhile, small amounts of two- and three-chain intermolecularly cross-linked SVEO were observed at smaller retention volumes. Again, judging from the much stronger peaks from free PEO at 21.1 mL for both samples, intramolecularly cross-linked SVEO again adsorbed onto the SEC columns because of the more exposed positive charges in the quarternized P2VP cores. The mobile phase was again changed to 0.05 M LiBr in DMF, and the corresponding results are shown in Figure 3. Single model peaks were observed at a retention volume of 18.8 mL, and peaks from intermolecularly cross-linked species became too small to be detectable. When the DBB-to-2VP molar ratio decreased to 1:2 (stoichiometric), intermolecular cross-linking with many (or poly) chains took place, resulting in a milky solution with strong Tyndall light scattering.

Second, when the temperature increased to 100 °C, intramolecular cross-linking was favored, as demonstrated in Figure 2B. When the DBB-to-2VP ratio was 8:1 and 2:1, intramolecular cross-linking of SVEO was obtained, as evidenced by single-model peaks at 19.2 mL. Their corresponding SEC curves in LiBr/DMF are shown in Figure 3. Sharp unimodel peaks with a slightly higher retention volume than that of SVEO were seen, implying successful synthesis of the intramolecularly cross-linked SVEO. When the DBB-to-2VP ratio was 1:2, intramolecular cross-linking of SVEO only partially took place, because a relatively broad peak was again observed between 18.6 and 19.2 mL.

For the above studies, excess DBB was not removed from the final reaction mixture before analysis. Therefore, it was possible that the excess DBB could further cause intermolecular cross-linking of the intramolecularly cross-linked SVEO. To eliminate this possibility, a control experiment was carried out for the intramolecularly cross-linked SVEO prepared at 100 °C with 2% polymer concentration and 2:1 DBB-to-2VP ratio. The DMF solvent was slowly evaporated at room temperature in a fume hood, followed by vacuum drying over a weekend. The DBB was completely removed as evidenced by the ^{1}H NMR study (see Results and Discussion below). After redissolving the dried/purified sample in DMF, SEC experiments with and without LiBr in the mobile phase were performed again, and the results are shown in Figures 2B and 3. Almost no changes in the SEC peaks were observed for the sample before and after removing the excess DBB, indicating that the solution property of the intramolecularly cross-linked samples in DMF would not be much affected by existence of excess DBB.

On the basis of the above results, we confirm that unimolecular Janus particles were successfully prepared due to effective intramolecular cross-linking of the SVEO triblock copolymer using DBB under specific reaction conditions. (1) When the temperature was at 30 °C, both high DBB-to-2VP molar ratio and high polymer concentration were required. (2) When the reaction was carried out at 100 °C, either relatively high DBB-to-2VP molar ratio or high polymer concentration was required. We speculate that the long PS and PEO end blocks form effective steric hindrance and can prevent cross-linking of the middle P2VP blocks from different chains in solution. This may be why the reaction can be carried out at a relatively high polymer concentration of 20 mg/mL. Meanwhile, the local concentration of the first quarternization product [Ar$-$N$^+$-(CH$_2$)$_4$Br] in the P2VP middle block also plays an important role. Assuming this concentration was far away from saturation (i.e., every 2VP unit is grafted with one DBB), the higher the concentration, the easier the second-step quarternization reaction for intramolecular cross-linking of the P2VP block. Finally, temperature is also important. The higher the reaction temperature, the easier the second-step quarternization reaction.

SLS and DLS Studies of Intramolecularly Cross-Linked SVEO. From the above SEC results, intramolecular cross-linking has been successfully achieved under unique cross-linking conditions with relatively high polymer concentration and/or high DBB-to-2VP ratios. However, the absolute molecular weight of the intramolecularly cross-linked SVEO needs to be quantitatively confirmed so that no chain scission and/or any other side reactions occurred. Because the weight fraction of aggregates of the intramolecularly cross-linked SVEO was very low at concentrations below 1.0 mg/mL (see SEC results above and discussion below), we used SLS to determine its absolute M_w. The Zimm plot for the intramolecularly cross-linked SVEO in DMF is shown in Figure 4, and a value of 352 000 g/mol was obtained. This M_w was slightly higher than that for the pure SVEO, suggesting that the smaller size (or hydrodynamic volume) particles must consist of single triblock copolymer chain. Because the intramolecularly cross-linked SVEO may be able to arrange its amphiphilic PS and PEO blocks at the opposite sides of the cross-linked P2VP core, the particle can be termed as a unimolecular polymeric Janus nanoparticle. Note that the slightly higher M_w could be attributed to the attachment, including both grafting and cross-linking, of DBB molecules to the middle P2VP block.

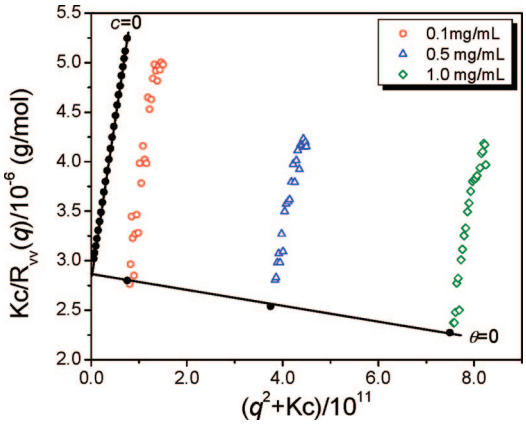

Figure 4. Zimm plot for the intramolecularly DBB-cross-linked SVEO triblock copolymer in DMF. The apparent second Viral coefficient A_2 is determined to be -2.86×10^{-4} mol·cm^3/g^2.

The size and size distribution of the unimolecular Janus nanoparticles at different concentrations during a gradual dilution procedure were characterized by DLS. Typical results are shown in Figure 5. Figure 5A shows the hydrodynamic radius *z*-distribution, $f_z(R_h)$. Two distinct peaks are always observed for a broad range of concentrations studied. The peak R_h values and the intensity ratio of the low to high R_h peaks are summarized in Table 1. Intriguingly, the smaller R_h values were kept almost the same, around 8.7 nm, while the larger R_h values gradually decreased from 115.6 nm at 20 mg/mL to 48.6 nm at 0.1 mg/mL. The smaller R_h could be attributed to the unimolecular Janus nanoparticle and the larger R_h must be their aggregates. The intensity ratio of the low to high R_h peaks increased from 0.8 to 3.1 upon decreasing the concentration, suggesting that large aggregates could dissociate into unimolecular Janus nanoparticles upon dilution. This indicates that they were physical instead of chemical aggregates. Figure 5B shows the hydrodynamic radius *w*-average distribution, $f_w(R_h)$, for the unimolecular Janus nanoparticles in DMF. Note that the *w*-average hydrodynamic radius distribution may reflect the weight fractions of different species in solution. Below 2.0 mg/mL, the weight fraction of large aggregates could be neglected, while above 2.0 mg/mL the weight fraction of large aggregates substantially increased. This is also consistent with SEC results in Figure 1B.

It is possible that ABC triblock copolymers may form aggregates even in a common solvent, as long as there is a substantial difference in the interactions between the solvent and different blocks. Figure 6A shows the *z*-average distribution of hydrodynamic radius for the pure SVEO in DMF. Above 2.0 mg/mL, two distinct peaks at different R_h values were observed (see also Table 1); the peak around 9.0 nm could be attributed to the single SVEO triblock molecule, while the peak around 45−62 nm was attributed to its aggregates. With decreasing the SVEO concentration, the intensity ratio of the low to high R_h peaks gradually increases (see Table 1), also implying the dissociation of the triblock aggregates. Below 0.5 mg/mL, a single peak was seen at approximately $R_h = 12$ nm. There are distinct differences between the pure and intramolecularly cross-linked SVEO samples. First, the pure SVEO had substantially smaller aggregate size than the unimolecular Janus nanoparticles at concentrations above 2.0 mg/mL. Second, even below 2.0 mg/mL, the unimolecular Janus nanoparticles still exhibited relatively large aggregates while the SVEO did not. Third, the weight fraction of aggregates for the pure SEVO was nearly negligible at all concentrations studied, and this is demonstrated in the hydrodynamic radius *w*-average distribution in Figure 6B. We therefore conclude that intramolecular cross-linking of the SVEO has substantially changed its solution property in the common solvent, DMF.

Morphology Study of Unimolecular Janus Nanoparticles and Their Aggregates. The morphologies of unimolecular polymeric Janus nanoparticles in dilute solutions and their aggregates in relatively concentrated solutions were studied by TEM. In Figure 7A, unimolecular polymeric Janus nanoparticles were clearly observed when the initial solution concentration during TEM sample preparation was 0.01 mg/mL. Note that because the evaporation of DMF at room temperature was fairly slow, much lower initial concentration of the solutions had to be used to avoid any aggregation of unimolecular polymeric nanoparticles during the solvent evaporation process. First, the dark spherical core was assigned as DBB-cross-linked P2VP because bromine has a higher electron density. Second, different overall shapes of the unimolecular polymeric Janus nanoparticles were seen after drying the samples on carbon-coated TEM grids. Note that these shapes resulted after preferential adsorption of unimolecular Janus nanoparticles onto the carbon film surface. Therefore, they may not exactly represent the molecular conformation in the DMF solution. At position I, the DBB-cross-linked P2VP cores are at one side of the unimolecular particle. In the inset of Figure 2A, a dumbbell on the left was observed with the DBB-cross-linked P2VP core between PS and PEO chains. For the other unimolecular nanoparticle on the right of the inset image, the DBB-cross-linked P2VP core was surrounded by PS and PEO chains. Because RuO_4 stains both PS and PEO blocks, we cannot differentiate them in these TEM images.

When the initial solution concentration increased to 0.25 mg/mL, supermicelles were observed after slow DMF evaporation at room temperature (see Figure 7B). Here, only aggregated supercores (gray) with a few (five to seven) dark DBB-cross-linked P2VP cores were seen. Because the shells must be highly solvated in DMF, the collapsed shells had a low density after solvent evaporation and thus appeared very light in the TEM micrograph. This is confirmed by an AFM study shown in Figure 8, where closely packed supermicelles are clearly seen. From the top topology of this AFM image, one can also see that one supermicelle consists of several smaller particles, which is consistent with the above TEM observation.

The average size of supermicelles was determined from TEM image analysis in Figure 9. A fast Fourier transform of the TEM

Table 1. DLS Results of R_h Values and the Intensity Ratio of the Low to High R_h Peaks for the Pure SVEO and DBB-Cross-Linked SVEO Janus Nanoparticles at Different Concentrations in DMF

	SVEO triblock copolymer			DBB-cross-linked SVEO		
concn (mg/mL)	R_h (nm)		peak intensity ratio	R_h (nm)		peak intensity ratio
20	8.6	62.2	1.3	7.9	115.6	0.8
10	8.9	54.0	1.3	8.5	99.2	0.5
5.0	9.3	45.6	1.5	9.3	70.3	1.8
2.0	9.5	49.5	2.5	9.4	58.3	2.4
0.5		12.8	−	9.3	48.3	1.8
0.1		11.3	−	8.8	48.6	3.1

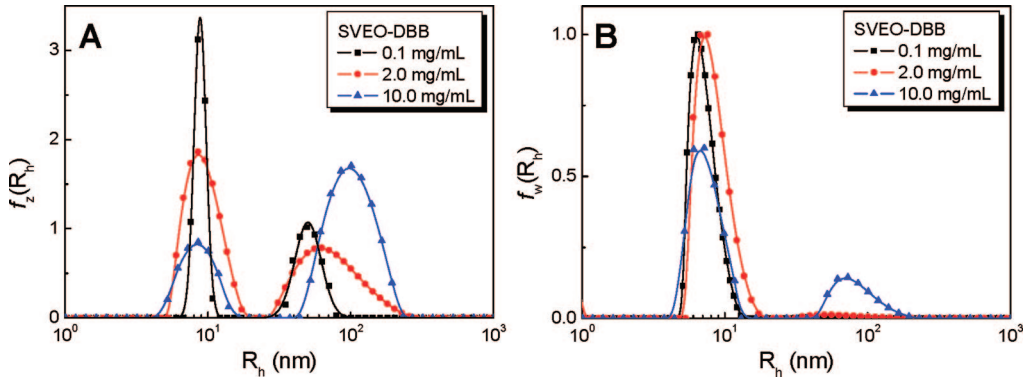

Figure 5. (A) *Z*- and (B) *w*-average distribution of the hydrodynamic radius for intramolecularly DBB-cross-linked SVEO at 0.1, 2.0, and 10 mg/mL, respectively.

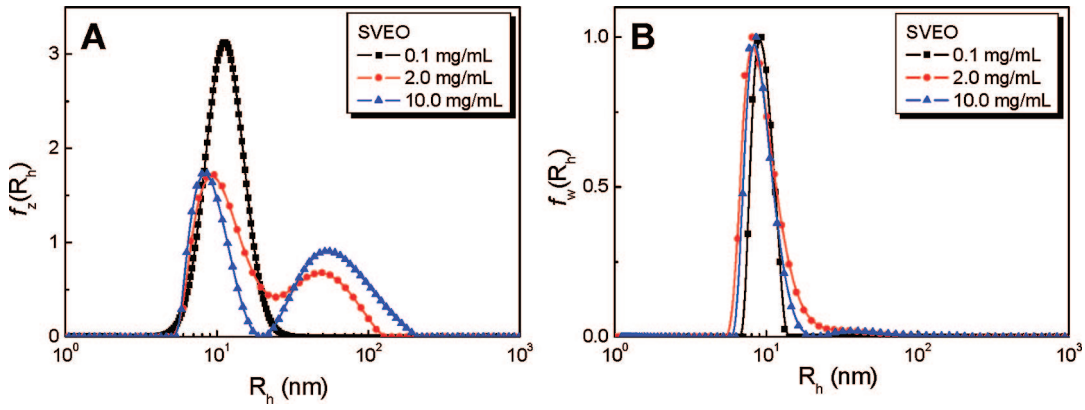

Figure 6. (A) *Z*- and (B) *w*-average distribution of the hydrodynamic radius for the pure SVEO at 0.1, 2.0, and 10 mg/mL, respectively.

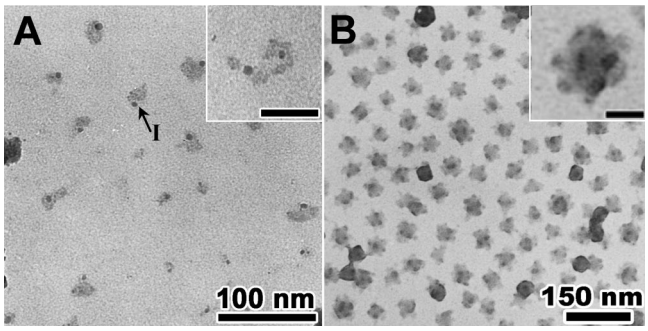

Figure 7. Bright-field TEM micrographs for the DBB-cross-linked SVEO: (A) unimolecular Janus nanoparticles and (B) their supermicelles, at initial solution concentrations of 0.01 and 0.25 mg/mL, respectively. Magnified images are shown as insets, and the scale bars in both insets are 50 nm. Sample in panel A was stained by RuO_4 for 15 min.

image in Figure 7B produced a diffraction image in the inset of Figure 9 showing two diffuse rings. After integration, these diffuse rings corresponded to average *d*-spacings of 75 and 22 nm, respectively. We attributed the spacing of 75 nm to the average size of close-packed supermicelles, which is further confirmed by an AFM line profile analysis shown in the bottom panel of Figure 8. From this line profile, the average size of the supermicelles was between 70 and 90 nm, which is smaller than the $2R_h$ values obtained from the DLS study (see Table 1). We speculate that the supermicelles actually shrank after solvent evaporation on a solid substrate (either carbon films on a TEM grid or silicon wafers). The spacing of 22 nm could be attributed to the average distance between the DBB-cross-linked P2VP cores in the supermicelle cores (also see the inset of Figure 7B).

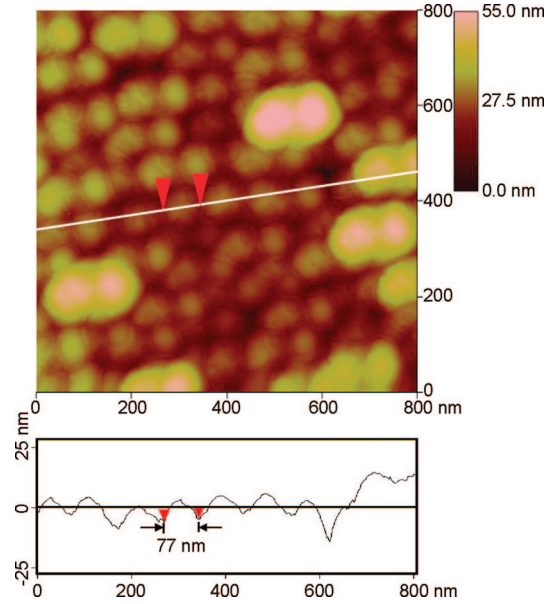

Figure 8. (Top) AFM height image of the closely packed unimolecular Janus nanoparticles on a silicon wafer substrate. (Bottom) The line profile as indicated in the top panel.

Judging from the solubility parameters for DMF, PS, and PEO (22.1, 17.8, and 20.3 $J^{1/2}\cdot cm^{-3/2}$),[64] respectively, PEO should form the corona, and PS should form the supercores. DBB-cross-linked P2VP nanoparticles should locate between the PS supercore and the PEO corona. This speculation is supported by ^1H NMR in DMF-d_7 (see Figure 10). For the pure SVEO (spectrum A) and its mixture with DBB at a molar ratio of DBB/2VP = 8:1 (spectrum B), all resonance peaks for PS (7.1 and

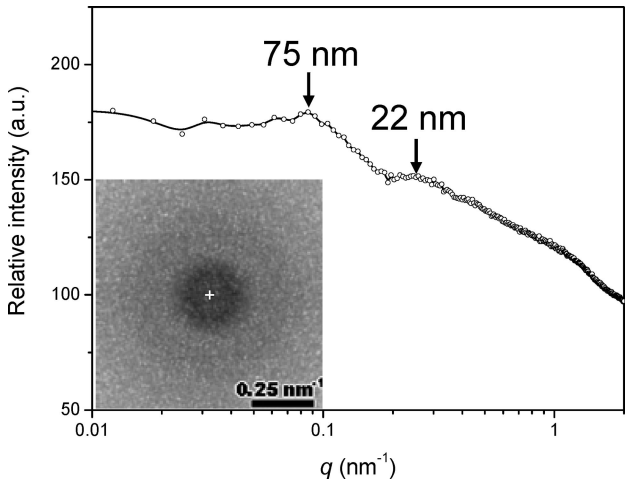

Figure 9. Integrated intensity curve from the two-dimensional fast Fourier transform image (the inset) of the TEM image in Figure 7B.

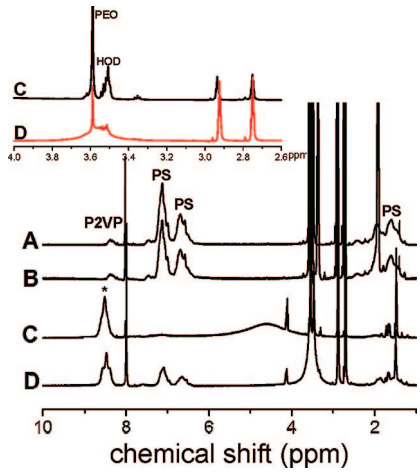

Figure 10. ^{1}H NMR spectra in DMF-d_7: pure SVEO (A), SVEO and DBB mixture at a ratio of 1:8 (B), and DBB-cross-linked SVEO at concentrations of (C) 20 mg/mL and (D) 2 mg/mL, respectively. The inset at the top shows expanded spectra for C and D in a range of 4.0−2.6 ppm. Peaks for PS (7.1 and 6.7 ppm), P2VP (8.4, 7.5, 7.1, and 6.7 ppm), and PEO (3.7 ppm) are labeled in the spectra. DMF peaks are located at 2.75, 2.92, and 8.03 ppm with a HOD peak at 3.5 ppm. DBB peaks in B are located at 1.9 and 3.3 ppm. After quarternization of P2VP, the DBB methylene peaks changed to 1.5 and 4.2 ppm, respectively, in C and D. The peak labeled with an asterisk is attributed to an unknown peak (see discussion in the text).

6.7 ppm), P2VP (8.4, 7.5, 7.1, and 6.7 ppm), and PEO (3.7 ppm) were present. At a low concentration of 2.0 mg/mL, chemical shifts for both PS and PEO blocks were observed (see spectrum D). However, at a high concentration of 20 mg/mL, chemical shifts for PS became very weak while that for PEO was retained (see spectrum C). This indicated that both PS and PEO were soluble in dilute solutions, while at high concentrations PEO formed the corona and PS formed the supercores. This unique self-assembly in a common solvent is similar to previous reports for other Janus particles[51,65] and Janus disks.[53]

The broad peak centered at 4.5 ppm in spectrum C is attributed to the Ar−N^+CH_2 peak in the quarternized (both grafted and cross-linked) P2VP with limited solubility and thus poor mobility, and the sharp peak at 4.2 ppm is attributed to the CH_2N^+ peak in the soluble quarternized P2VP moieties with good mobility. For a detailed explanation for different resonance peaks, refer to the discussion of Figure S1 in the Supporting Information. The cross-linking density vs grafting density for the final product can be estimated from spectrum C in Figure 10. When DBB was grafted, the relatively weak Ar−$N^+CH_2CH_2CH_2CH_2$Br peak was found at 3.3 ppm. When DBB is cross-linked/grafted, the relatively strong Ar−N^+CH_2-$CH_2CH_2CH_2N^+$−Ar and Ar−$N^+CH_2CH_2CH_2CH_2$Br peaks were overlapped at 1.5 ppm. After integration, the cross-linking to grafting ratio was estimated to be 7:2. Therefore, the effect of DBB grafting was negligible and did not disturb the molecular design of the unimolecular Janus nanoparticles.

We also note that after DBB cross-linking of the middle P2VP block, a strong resonance peak was seen at 8.6 ppm. Two control quarternization experiments were carried out for a P2VP homopolymer and a PS-*b*-P2VP diblock copolymer, respectively (see Figures S1 and S2 in the Supporting Information, respectively). For the P2VP homopolymer, the polymer precipitated after 100% quarternization, while no precipitation was observed for the PS-*b*-P2VP diblock copolymer. However, after complete quarternization of the 2VP units, all P2VP peaks disappeared and a relatively strong triplet peak emerged at 8.5 ppm for both samples. The exact reason for the appearance of the peak at 8.5 ppm after P2VP quarternization is still unclear and needs further investigation.

On the basis of the above results, it is obvious that by simple chemical cross-linking of the middle P2VP blocks in SVEO, unimolecular polymeric Janus nanoparticles were successfully obtained using DBB as the cross-linking agent at relatively high polymer concentration and high DBB-to-2VP ratios, and they exhibited intriguing concentration-dependent aggregation behavior in a common solvent. As discussed above, during the reaction of DBB with SVEO, three events are possible, namely, grafting of DBB molecules to the P2VP block and intra- and intermolecular cross-linking of the middle P2VP blocks. First, the fast first-step quarternization (or grafting) reaction shall be avoided, because cross-linker grafting onto P2VP would result, given that the cross-linker is in an excess in most cases. As a result, 1,4-diiodobutane was not used in this study to prepare unimolecular polymeric Janus nanoparticles. Second, the second-step quarternization (cross-linking) reaction should be relatively fast. This is why high DBB-to-2VP molar ratio was efficient for intramolecular cross-linking. Third, the soluble and long PS and PEO chains effectively shielded the middle P2VP block and avoided intermolecular cross-linking during the reaction. We speculate that this might be the reason why unimolecular polymeric Janus nanoparticles could be achieved even when the triblock copolymer concentration was as high as 20 mg/mL. Therefore, large quantity preparation of unimolecular polymeric Janus nanoparticles is made practical. Fourth, after cross-linking of the P2VP middle blocks, the apparent solvent quality regarding the whole triblock copolymer changed, because the apparent second Viral coefficient A_2 changed from 3.41×10^{-4} mol·cm^3/g^2 for the pure SVEO to -2.86×10^{-4} mol·cm^3/g^2 for the unimolecular polymeric Janus nanoparticles (see Figures 1A and 4). Note that positive, zero, and negative A_2 values correspond to good, θ, and poor solvents, respectively.[66] In addition, the PS solubility parameter is the most different from that of DMF. Therefore, supermicelles could form with PS forming the core and PEO being the corona, when the concentration reached high enough. Eventually, DBB cross-linked P2VP located between the PS core and PEO corona (see Figure 7B).

Conclusions

In summary, unimolecular (the smallest) polymeric Janus nanoparticles were successfully prepared, in relatively large quantity, by cross-linking the middle P2VP blocks using DBB in DMF under unique conditions; high SVEO concentration and/or high DBB-to-2VP molar ratio. It was inferred that the relatively long PS and PEO end blocks effectively prohibited

intermolecular cross-linking. After intramolecular cross-linking of the middle P2VP block, DMF changed from a good solvent to a slightly poor solvent, as suggested by the fact that the A_2 changed from a positive value for the pure SVEO to a negative value for the unimolecular Janus nanoparticles. When the solution concentration gradually increased, self-assembly of the unimolecular polymeric Janus nanoparticles into supermicelles with an R_h of 50−115 nm was observed by DLS. Finally, our method to prepare polymeric Janus nanoparticles is not limited to a specific block copolymer composition required for the "sphere-on-the-wall" morphology.[9−12]

Acknowledgment. This work was supported by Natural Science Foundation of China (20528405 and 20574014) and NSF CAREER Award DMR-0348724.

Supporting Information Available: ^{1}H NMR spectra of P2VP and PS-*b*-P2VP quarternization with *n*-bromopentane and CH_3I in DMF-d_7 and UV−vis SEC results for DBB-cross-linked SVEO under different reaction conditions. This material is available free of charge via the Internet at http://pubs.acs.org.

References and Notes

(1) Davankov, V. A.; Ilyin, M. M.; Tsyurupa, M. P.; Timofeeva, G. I.; Dubrovina, L. V. *Macromolecules* **1996**, *29*, 8398–8403.
(2) Davankov, V. A.; Timofeeva, G. I.; Ilyin, M. M.; Tsyurupa, M. P. *J. Polym. Sci., Part A: Polym. Chem.* **1997**, *35*, 3847–3852.
(3) Mecerreyes, D.; Lee, V.; Hawker, C. J.; Hedrick, J. L.; Wursch, A.; Volksen, W.; Magbitang, T.; Huang, E.; Miller, R. D. *Adv. Mater.* **2001**, *13*, 204–208.
(4) Harth, E.; Van Horn, B.; Lee, V. Y.; Germack, D. S.; Gonzales, C. P.; Miller, R. D.; Hawker, C. J. *J. Am. Chem. Soc.* **2002**, *124*, 8653–8660.
(5) Cherian, A. E.; Sun, F. C.; Sheiko, S. S.; Coates, G. W. *J. Am. Chem. Soc.* **2007**, *129*, 11350–11351.
(6) Mackay, M. E.; Dao, T. T.; Tuteja, A.; Ho, D. L.; Van Horn, B.; Kim, H. C.; Hawker, C. J. *Nat. Mater.* **2003**, *2*, 762–766.
(7) Daniel, M. C.; Astruc, D. *Chem. Rev.* **2004**, *104*, 293–346.
(8) Zhang, Z.; Glotzer, S. C. *Nano Lett.* **2004**, *4*, 1407–1413.
(9) Glotzer, S. C. *Science* **2004**, *306*, 419–420.
(10) Zhang, Z.; Horsch, M. A.; Lamm, M. H.; Glotzer, S. C. *Nano Lett.* **2003**, *3*, 1341–1346.
(11) de Gennes, P. G. *Rev Mod. Phys.* **1992**, *64*, 645–648.
(12) Perro, A.; Reculusa, S.; Ravaine, S.; Bourgeat-Lami, E. B.; Duguet, E. *J. Mater. Chem.* **2005**, *15*, 3745–3760.
(13) Pickering, S. U. *J. Chem. Soc.* **1907**, *91*, 2001.
(14) Binks, B. P. *Curr. Opin. Colloid Interface Sci.* **2002**, *7*, 21–41.
(15) Sheridon, N. K.; Richley, E. A.; Mikkelsen, J. C.; Tsuda, D.; Crowley, J. C.; Oraha, K. A.; Howard, M. E.; Rodkin, M. A.; Swidler, R.; Sprague, R. *J. Soc. Inf. Disp.* **1999**, *7*, 141–144.
(16) Crowley, J. M.; Sheridon, N. K.; Romano, L. *J. Electrostatics* **2002**, *55*, 247–259.
(17) Takei, H.; Shimizu, N. *Langmuir* **1997**, *13*, 1865–1868.
(18) Casagrande, C.; Fabre, P.; Raphaël, E.; Veyssié, M. *Europhys. Lett.* **1989**, *9*, 251–255.
(19) Paunov, V. N.; Cayre, O. J. *Adv. Mater.* **2004**, *16*, 788–791.
(20) Lu, Y.; Xiong, H.; Jiang, X.; Xia, Y.; Prentiss, M.; Whitesides, G. M. *J. Am. Chem. Soc.* **2003**, *125*, 12724–12725.
(21) Hugonnot, E.; Carles, A.; Delville, M. H.; Panizza, P.; Delville, J. P. *Langmuir* **2003**, *19*, 226–229.
(22) Cayre, O.; Paunov, V. N.; Velev, O. D. *J. Mater. Chem.* **2003**, *13*, 2445–2450.
(23) Koo, H. Y.; Yi, D. K.; Yoo, S. J.; Kim, D. Y. *Adv. Mater.* **2004**, *16*, 274–277.
(24) Fujimoto, K.; Nakahama, K.; Shidara, M.; Kawaguchi, H. *Langmuir* **1999**, *15*, 4630–4635.
(25) Petit, L.; Sellier, E.; Duguet, E.; Ravaine, S.; Mingotaud, C. *J. Mater. Chem.* **2000**, *10*, 253–254.
(26) Gu, H.; Yang, Z.; Gao, J.; Chang, C. K.; Xu, B. *J. Am. Chem. Soc.* **2005**, *127*, 34–35.
(27) Hong, L.; Jiang, S.; Granick, S. *Langmuir* **2006**, *22*, 9495–9499.
(28) Suzuki, D.; Tsuji, S.; Kawaguchi, H. *J. Am. Chem. Soc.* **2007**, *129*, 8088–8089.
(29) Dendukuri, D.; Pregibon, D. C.; Collins, J.; Hatton, T. A.; Doyle, P. S. *Nat. Mater.* **2006**, *5*, 365–369.
(30) Nie, Z.; Li, W.; Seo, M.; Xu, S.; Kumacheva, E. *J. Am. Chem. Soc.* **2006**, *128*, 9408–9412.
(31) Shepherd, R. F.; Conrad, J. C.; Rhodes, S. K.; Link, D. R.; Marquez, M.; Weitz, D. A.; Lewis, J. A. *Langmuir* **2006**, *22*, 8618–8622.
(32) Roh, K. H.; Martin, D. C.; Lahann, J. *Nat. Mater.* **2005**, *4*, 759–763.
(33) Li, Z.; Lee, D.; Rubner, M. F.; Cohen, R. E. *Macromolecules* **2005**, *38*, 7876–7879.
(34) Giersig, M.; Ung, T.; LizMarzan, L. M.; Mulvaney, P. *Adv. Mater.* **1997**, *9*, 570–575.
(35) Gu, H.; Zheng, R.; Zhang, X.; Xu, B. *J. Am. Chem. Soc.* **2004**, *126*, 5664–5665.
(36) Teranishi, T.; Inoue, Y.; Nakaya, M.; Oumi, Y.; Sano, T. *J. Am. Chem. Soc.* **2004**, *126*, 9914–9915.
(37) Yu, H.; Chen, M.; Rice, P. M.; Wang, S. X.; White, R. L.; Sun, S. *Nano Lett.* **2005**, *5*, 379–382.
(38) Perro, A.; Reculusa, S.; Pereira, F.; Delville, M. H.; Mingotaud, C.; Duguet, E.; Bourgeat-Lami, E.; Ravaine, S. *Chem. Commun.* **2005**, 5542–5543.
(39) Sung, K. M.; Mosley, D. W.; Peelle, B. R.; Zhang, S.; Jacobson, J. M. *J. Am. Chem. Soc.* **2004**, *126*, 5064–5065.
(40) Huo, Q.; Worden, J. G. *J. Nanoparticle Res.* **2007**, *9*, 1013–1025.
(41) Liu, X.; Worden, J. G.; Dai, Q.; Zou, J.; Wang, J.; Huo, Q. *Small* **2006**, *2*, 1126–1129.
(42) Worden, J. G.; Dai, Q.; Shaffer, A. W.; Huo, Q. *Chem. Mater.* **2004**, *16*, 3746–3755.
(43) Worden, J. G.; Shaffer, A. W.; Huo, Q. *Chem. Commun.* **2004**, 518–519.
(44) Zou, J.; Dai, Q.; Wang, J.; Liu, X.; Huo, Q. *J. Nanosci. Nanotechnol.* **2007**, *7*, 2382–2388.
(45) Li, B.; Li, C. Y. *J. Am. Chem. Soc.* **2007**, *129*, 12–13.
(46) Shaffer, A. W.; Worden, J. G.; Huo, Q. *Langmuir* **2004**, *20*, 8343–8351.
(47) Alivisatos, A. P.; Johnsson, K. P.; Peng, X.; Wilson, T. E.; Loweth, C. J.; Bruchez, M. P.; Schultz, P. G. *Nature* **1996**, *382*, 609–611.
(48) Loweth, C. J.; Caldwell, W. B.; Peng, X.; Alivisatos, A. P.; Schultz, P. G. *Angew. Chem., Int. Ed.* **1999**, *38*, 1808–1812.
(49) Walther, A.; Müller, A. H. E. *Soft Matter* **2008**, *4*, 663–668.
(50) Saito, R.; Fujita, A.; Ichimura, A.; Ishizu, K. *J. Polym. Sci., Part A: Polym. Chem.* **2000**, *38*, 2091–2097.
(51) Erhardt, R.; Boker, A.; Zettl, H.; Kaya, H.; Pyckhout-Hintzen, W.; Krausch, G.; Abetz, V.; Müller, A. H. E. *Macromolecules* **2001**, *34*, 1069–1075.
(52) Liu, Y.; Abetz, V.; Müller, A. H. E. *Macromolecules* **2003**, *36*, 7894–7898.
(53) Walther, A.; Andre, X.; Drechsler, M.; Abetz, V.; Müller, A. H. E. *J. Am. Chem. Soc.* **2007**, *129*, 6187–6198.
(54) Walther, A.; Hoffmann, M.; Müller, A. H. E. *Angew. Chem., Int. Ed.* **2008**, *47*, 711–714.
(55) Xu, H.; Erhardt, R.; Abetz, V.; Müller, A. H. E.; Goedel, W. A. *Langmuir* **2001**, *17*, 6787–6793.
(56) Erhardt, R.; Zhang, M. F.; Boker, A.; Zettl, H.; Abetz, C.; Frederik, P.; Krausch, G.; Abetz, V.; Müller, A. H. E. *J. Am. Chem. Soc.* **2003**, *125*, 3260–3267.
(57) Forster, S.; Abetz, V.; Müller, A. H. E. *Adv. Polym. Sci.* **2004**, *166*, 173–210.
(58) Mori, H.; Müller, A. H. E. *Prog. Polym. Sci.* **2003**, *28*, 1403–1439.
(59) Gohy, J. F.; Khousakoun, E.; Willet, N.; Varshney, S. K.; Jerome, R. *Macromol. Rapid Commun.* **2004**, *25*, 1536–1539.
(60) Li, G.; Shi, L.; Ma, R.; An, Y.; Huang, N. *Angew. Chem., Int. Ed.* **2006**, *45*, 4959–4962.
(61) Nie, L.; Liu, S.; Shen, W.; Chen, D.; Jiang, M. *Angew. Chem., Int. Ed.* **2007**, *46*, 6321–6324.
(62) Chen, D.; Peng, H.; Jiang, M. *Macromolecules* **2003**, *36*, 2576–2578.
(63) Zhu, L.; Cheng, S. Z. D.; Calhoun, B. H.; Ge, Q.; Quirk, R. P.; Thomas, E. L.; Hsiao, B. S.; Yeh, F.; Lotz, B. *Polymer* **2001**, *42*, 5829–5839.
(64) Brandup, J.; Immergut, E. H.; Grulke, E. A. *Polymer Handbook*, 4th ed.; Wiley-Interscience: New York, 1999.
(65) Hong, L.; Cacciuto, A.; Luijten, E.; Granick, S. *Nano Lett.* **2006**, *6*, 2510–2514.
(66) Flory, P. J. *Principles of Polymer Chemistry*; Cornell University Press: Ithaca, NY, 1953.

MA800461Z